Supporting information

Experimental section

Chemicals

$ZnCl_2$, $CuSO_4$, $CaCl_2$, $MgCl_2$, $NiCl_2$, $MnCl_2$, $CdCl_2$, $CoCl_2$, $FeCl_2$, $FeCl_3$, $AgNO_3$, NaCl, KCl were purchased from Shanghai Zhenxin Reagent Company. Tetrakis(acetonitrile) copper(I) hexafluorophosphate used as the copper(I) source for *in vitro* experiment, was purchased from J&K Chemical Ltd. KCN was kindly provided by Prof. Jinlin Zuo of the School of Chemistry and Chemical Engineering, Nanjing University. All chemicals are of analytical grade and were used directly without further purification.

Sequence of EGFP145-Amt1

MVSKGEELFTGVVPILVELDGDVNGHKFSVSGEGEGDATYGKLTLKFICTTGKLPVPWP
TLVTTLTYGVQCFSRYPDHMKQHDFFKSAMPEGYVQERTIFFKDDGNYKTRAEVKFEG
DTLVNRIELKGIDFKEDGNILGHKLEYNlg***RGRPPTTCDHCKDMRKTKNVNPSGSCNCSK***
LEKIRQEKGITIEEDMLMSGNMDMCLCVRGEPCRCHARRKRTQKSlgYNSHNVYIMADK
QKNGIKVNFKIRHNIEDGSVQLADHYQQNTPIGDGPVLLPDNHYLSTQSALSKDPNEKRD
HMVLLEFVTAAGITLGMDELYK

The sequence of Amt1 copper(I) binding domain is highlighted in italic and bold.

Construction of the expression plasmid

pet32a-EGFP plasmid was generously provided by Ms. Wei Wang in the School of Life Science, Nanjing University. Amt1 copper(I) binding domain in the pcDNA3.1(+) plasmid was a generous gift from Prof. Chuan He of the University of Chicago. The EGFP sequence was amplified using polymerase chain reaction (PCR) and inserted into pUC19 vector in between BamHI and KpnI sites for sensor engineering.

In order to prepare the chimera protein with Amt1 copper(I) binding domain inserted into EGFP between residue 145 and 146, a palindromic AvaI restriction site was introduced into this site through site-directed mutagenesis PCR, resulting in pUC19-EGFP(AvaI). Then AvaI restriction site was also introduced to both ends of the Amt1 sequence using PCR. The Amt1 sequence was digested by AvaI and subcloned into pUC19-EGFP(AvaI) that was linearized by AvaI digestion. This yielded the full length gene of the sensor protein EGFP-145Amt1 in pUC19 vector. Then the senor gene was transferred into pQE80L vector for expression. The full length gene was confirmed by direct sequencing.

The Amt1 sequence was also inserted into pQE80L vector in between BamHI and KpnI sites for the expression of Amt1 in *E. coli*.

Protein expression and purification

pQE80L-eGFP145Amt146 was transformed into *E.coli* BL21. Each clone harboring a corresponding plasmid was grown in 2.5% LB medium containing 100 mg/L ampicillin under vigorous stirring (225 rpm), and induced with 1mM isopropyl-1-β-D-thiogalactoside (IPTG) when its optical density (OD) at 600 nm reached ~0.6-0.8. Protein expression continued for 6 hours at 28 ^{o}C. The cells were harvested by centrifugation and resuspended in pre-cooled lysis buffer (20 mM Na_3PO_4, 500 mM NaCl, 4 mM DTT, pH 7.4)), further lysed by 100μM lysozyme and sonicated on ice for 8 min. Then the cell lysate was centrifuged at 12000 rpm for 30 min at 4

^{o}C. The protein is purified using Ni^{2+}-NTA protein resin (GE healthcare, Shanghai) and eluted in elution buffer (20 mM Na_3PO_4, 500 mM NaCl, 4 mM DTT, 500 mM imidazole, pH 7.4). The purified protein is dialyzed against a buffer containing 10 mM Tris-HCl, 300 mM NaCl, 4 mM DTT (pH 7.4). Typically, 40-50 mg of protein was obtained from 1 L of LB medium.

pQE80L-Amt1 was transformed into BL21 cell. Each clone harboring a corresponding plasmid was grown in 2.5% LB medium containing 100 mg/L ampicillin under vigorous stirring (225rpm) at 37^{o}C until OD at 600 nm reached ~0.6-0.8, then the temperature was lowered to 22^{o}C. Protein expression was induced by 0.5mM IPTG. 1.4mM $CuSO_4$ was added to the growth medium half hour after the induction to provide the copper(I) source for the correct folding of Amt1. The cells were allowed to grow for another 5 hours. The purification protocol was the same as purifying sensor protein. For the generation of apo-Amt1, 4mM neocuproine was added to the purified Amt1, and then removed by dialysis against pure water.

Far-UV Circular Dichroism (CD)

CD spectra were measured using a JASCO J-810 or J-815 CD spectropolarimeter (Jasco, Japan). Protein samples were first desalted by dialysis against pure water. Then desired amount of metal ions were added and equilibrated for 20 min before measurement. The data were recorded with a wavelength scan from 250 to 190 nm at room temperature with a quartz cell of 0.1 mm path length. The data reported in the paper were averaged from at least 5 scans to improve the signal-to-noise ratio and the contribution from buffer was subtracted. Results are expressed as mean residue ellipticity (θ_{MRE}), calculated according to Equation (1), where θ_{obs} is the observed ellipticity (in deg), d is pathlength (in cm), C is concentration of protein samples (M), and n is total number of amino acids in the protein.

$$\theta_{MRE} = (100\ \theta_{obs})/[dC(n-1)] \quad (1)$$

For the thermal melting experiment, the temperature ramp was 5^{o}C/min and the CD signal at 215 nm was monitored.

Fluorescence measurement

The fluorescence measurement was done on a fluorescence spectrophotometer (JASCO FP-6500), with an excitation wavelength of 400 nm. Protein concentration was kept constant at 1μM for all measurements. The molar ratio of copper(I) over sensor protein varied from 1 to 5. The excitation and emission bandwidth were set to be 10 nm and 5 nm, respectively.

The normalized fluorescence intensity refers to the fluorescence of the sensor at various wavelength divided by the maximum fluorescence intensity.

The normalized fluorescence change equals the fluorescence of the sensor at certain copper(I) concentration divided by the fluorescence difference of the apo and holo form sensor.

Estimation of dissociation constant from competitive binding assay

To estimate the dissociation constant of copper(I) to EGFP-145Amt1, 0.5μM holo-EGFP-145Amt1 is prepared. Then different amount of NaCN is added into the samples to replace the bound copper(I), thus restoring the fluorescence (Fig. 2b). The equilibrium constants in this solution are as following based on *NIST Critical Stability Constants of Metal Complexes*:

$$H^+ + CN^- \leftrightarrow HCN \qquad \log K_a = 9.04$$
$$Cu^+ + 2CN^- \leftrightarrow Cu(CN)_2^- \qquad \log \beta_{2Cu} = 21.7$$
$$Cu^+ + 3CN^- \leftrightarrow Cu(CN)_3^{2-} \qquad \log \beta_{3Cu} = 26.8$$
$$Cu^+ + 4CN^- \leftrightarrow Cu(CN)_4^{3-} \qquad \log \beta_{4Cu} = 27.9$$

Then, The log beta of EGFP-145Amt1 with copper(I) was estimated using HySS2009 software.

UV-Vis measurement

UV-Vis spectra of sensor protein in the absence and presence of copper(I) were taken using a UV/VIS spectrophotometer (Jasco, V-550) at a sensor concentration of 15 μM in a buffer containing 10 mM Tris-HCl, 300 mM NaCl and 4 mM DTT (pH 7.4). For the measurement of sensor bound with copper(I), additional 60 μM copper(I) was present. The contribution from the buffer has been subtracted.

The characterization of the stability of sensor protein and Amt1

The thermodynamic stability of sensor protein and Amt1 in the presence and absence of copper(I) was measured using guanidinium hydrochloride denaturation. Fluorescence at 515 nm was used to monitor the unfolding of the sensor protein, and CD ellipticity at 222 nm was used to monitor the unfolding of Amt1.

The chemical denaturation data were fitted to the following equation:

$$F = \frac{\exp((m \cdot [D] - \Delta G_{D-N}^{H_2O}) / RT)}{1 + \exp((m \cdot [D] - \Delta G_{D-N}^{H_2O}) / RT)} \qquad (3)$$

Where F is the fraction of unfolded proteins, m is the slope of the transition, [D] is the concentration of the denaturant, $\Delta G_{D\text{-}N}^{H2O}$ is the free energy of unfolding in the absence of denaturant, R is the gas constant and T is the absolute temperature in Kelvin.

Living cell fluorescence imaging

CHO cells were incubated at 37 ^{o}C under 5% CO_2 in DMEM (Hyclone) supplemented with 10% FBS. For the expression ofEGFP-145Amt1, CHO cells were seeded overnight into 6-well coverslip-bottom culture chambers (Nunc) to obtain 85-90% confluency. The following day, the cells were transfected with pcDNA3.1(-) carrying the EGFP-145Amt1 gene using Lipofectamine 2000 (Invitrogen) according to the manufacturer's protocol. After allowing a 24 hr expression period, the cells were used for imaging. Videos and images were taken using an inverted fluorescence microscope (Olympus BX51 with Olympus DP72 Microscope Digital Camera System, Olympus Corp., Shinjuku-ku, Tokyo, Japan) equipped with a 100 ×objective, NA 1.35. 1 mM $CuSO_4$ was added to the growth medium to image the fluorescence changes in CHO cell. In

the control experiment, 1 mM $ZnCl_2$ was added to the medium. Images were collected and analyzed with Image-pro Express 6.3 (Media Cybernetics, Inc., Bethesda, Maryland, USA, http://www.mediacy.com/, 1981-2011).

Based on our *in vitro* experiments, the relationship between normalized fluorescence change and time can be described as pseudo first order kinetics.

$$Y=Aexp(-k*t) \quad (4)$$

Where Y is the normalized fluorescence intensity, A is the prefactor, *k* is the fluorescence change rate.

Therefore,

$$-\frac{\frac{dY}{dt}}{Y} = -\frac{-k*Aexp(-k*t)}{Aexp(-k*t)} = k \quad (5)$$

In Figure 4l, the –dY/dt/Y is plotted against time to reflect the fluorescence change rate over time.

Since the fluorescence quenching rate is directly related to the concentration of copper(I), we were able to use the fluorescence decrease rate in Fig. 4l as a reporter for the concentration of copper(I) in vivo based on the calibration curve shown in Fig. 2c, inset. The maximum copper concentration in the cell is estimated in the range of 10- 20 μM, which is significantly higher than typically copper concentrations in cells.

We smoothed our data by moving average of 10 consecutive points before taking the derivative of the curves in Fig. 4k. Otherwise the high noise level can cause artifacts. For example, the oscillations of the data at time longer than 100 seconds in Fig. 4l are indeed originated from the low signal-to-noise ratio at this region.

The fluorescence change inside the cells is also reversible. The fluorescence of the cells can be partially recovered (to ~80% of its original intensity) by washing away the copper(II) in the medium and adding 2 mM neocuproine.

Supporting figures

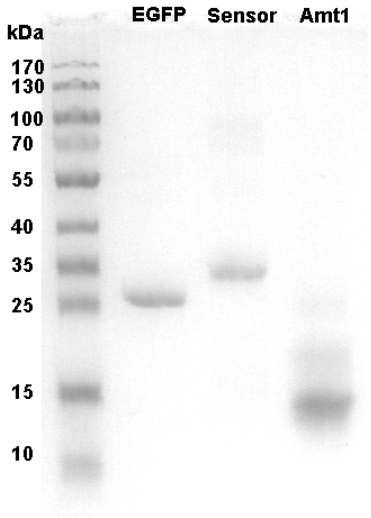

Fig. S1. SDS-PAGE of Protein ladder, EGFP, sensor protein (EGFP-145Amt1) and Amt1 (from left to right)

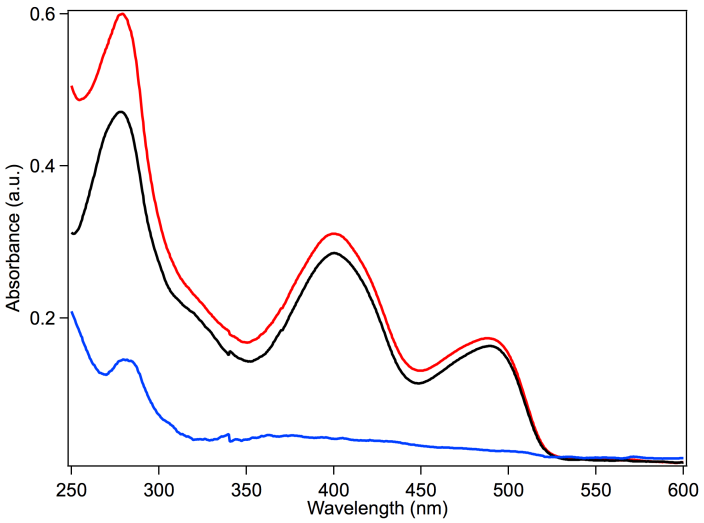

Fig. S2. UV spectra of sensor protein in the absence (black) and presence (red) of copper(I). The difference between these two spectra is shown in blue. The increased absorbance at ~280 nm is due to the formation of copper(I)-thiol clusters. Moreover, the peak at ~400 nm does not shift upon adding copper(I), suggesting a large proportion of protonated chromophore in the sensor protein which does not change upon copper(I) binding. It is worth noting that the peak at ~400 nm is not present in EGFP but in wt GFP, suggesting that the pKa of the sensor protein shifts towards that of the wt GFP.

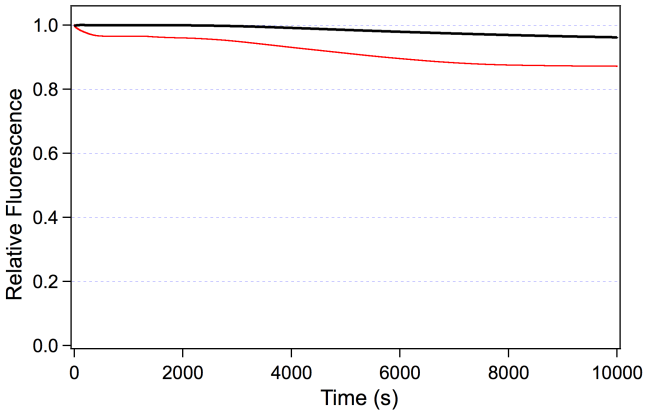

Fig. S3. Photo stability of the apo form EGFP-145Amt1 (Red) and wild type EGFP (Black) in Tris buffer (pH 7.4) using a Jasco fluorescence photospectometer under 0.2mW/cm^2 excitation at 400 nm (excitation bandwidth: 1 nm).

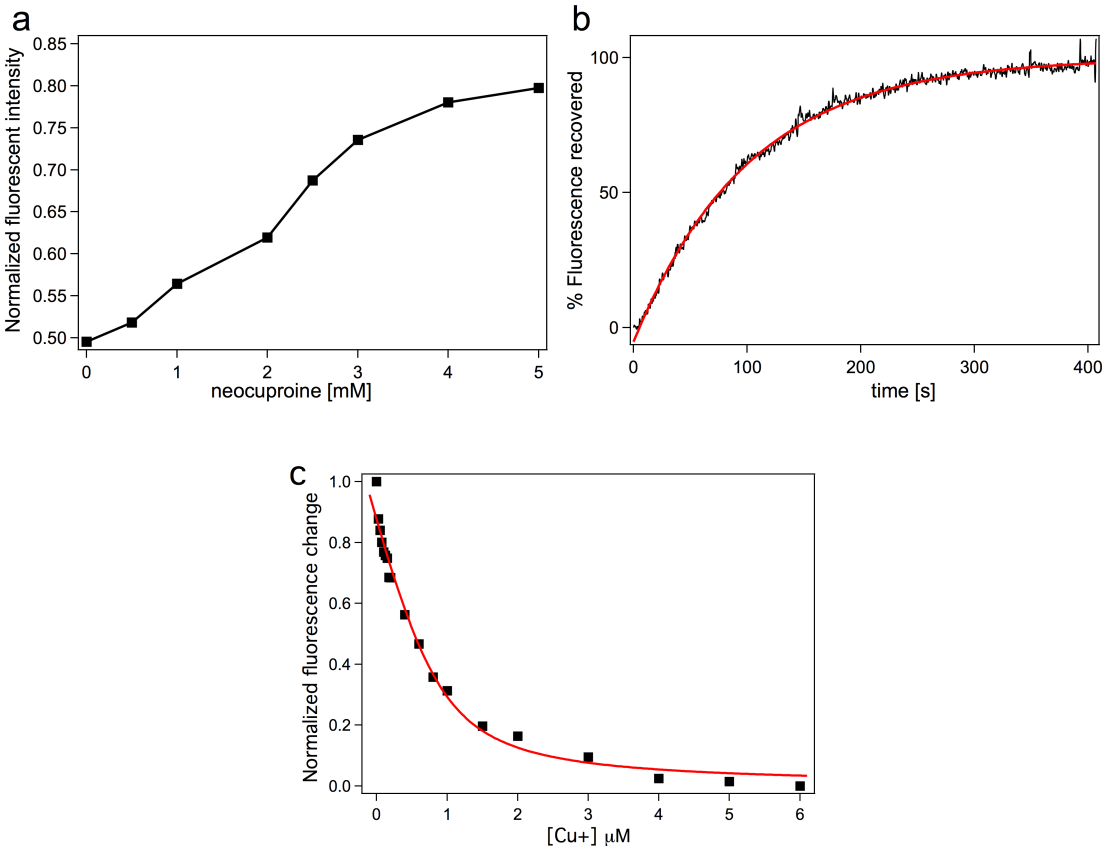

Fig. S4. a) The fluorescence of the sensor protein (1μM) can be recovered by adding copper(I) chelator, neocuproine. b) The fluorescence recovering kinetics upon adding 4 mM neocuproine. The recovery rate is 0.01 s^{-1} at this condition. c) The quenching of the fluorescence of the sensor upon adding various concentrations of copper(I) ions.

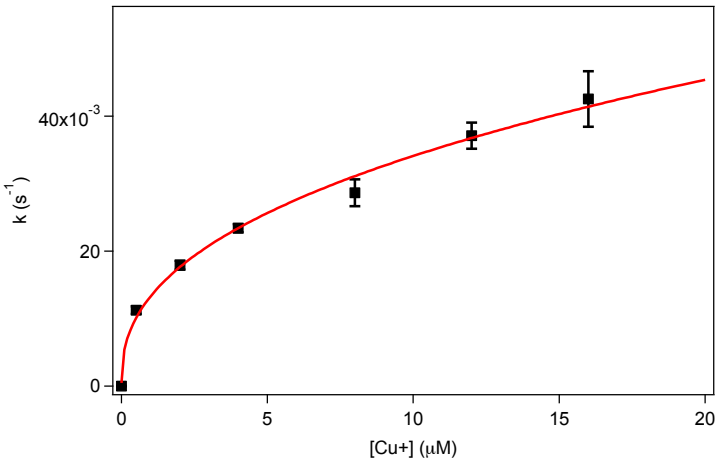

Fig. S5. The rate of fluorescence change of sensor protein at 5 nM upon adding various concentrations of copper(I). At these conditions, copper(I) is in large excess.

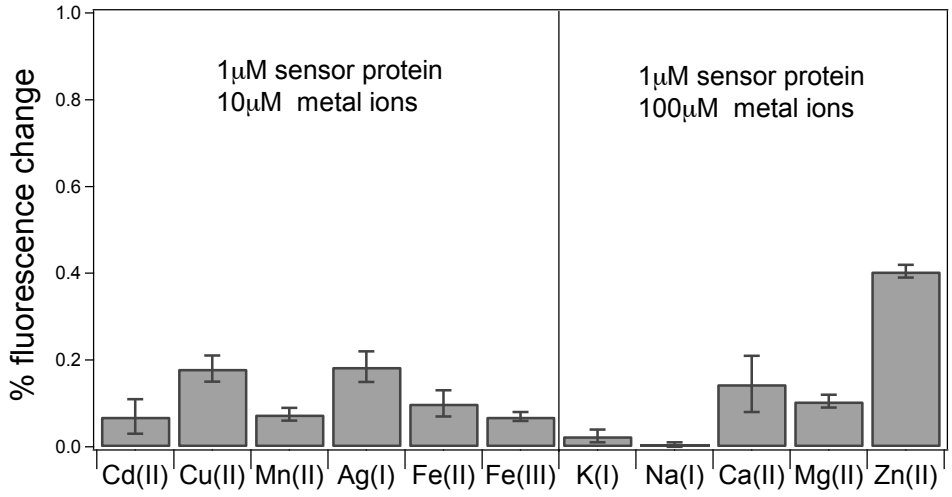

Fig. S6. Fluorescence change of sensor protein upon adding higher concentration of metal ions.

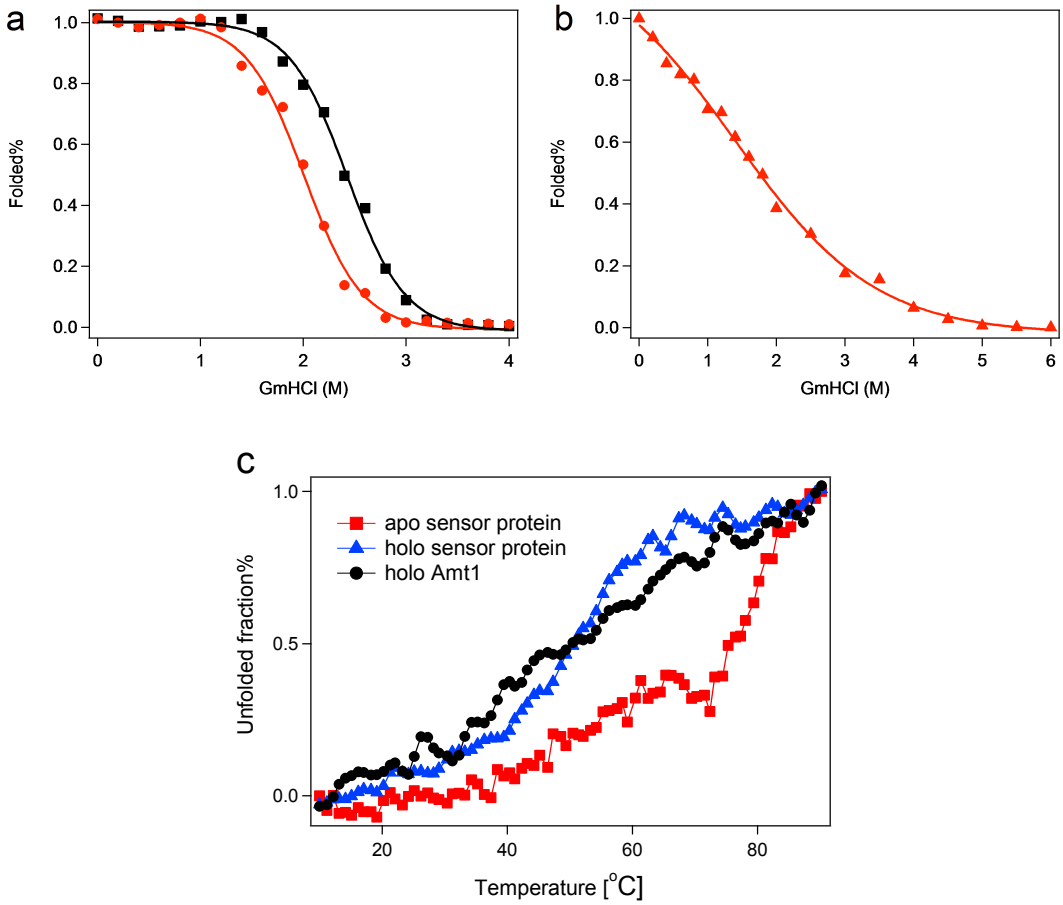

Fig. S7. The thermodynamic stability of sensor protein and Amt1. a) The thermodynamic stability of sensor protein decreases upon binding to copper(I). Black and red symbols corresponds to the sensor protein in the absence and presence of 4 equiv. of copper(I), respectively. Fluorescence at 515 nm was used to monitor the unfolding of the sensor protein, and CD ellipticity at 222 nm was used to monitor the unfolding of Amt1. The apo Amt1 does not show any detectable thermodynamic stability. b) The thermodynamic stability of Amt1 in the presence of 4 equiv. of copper(I). c) Thermodynamic stability of sensor protein and Amt1 measured thermal melting monitored by the CD signal change at 222 nm. Protein concentrations for all measurements were 1 μM throughout.

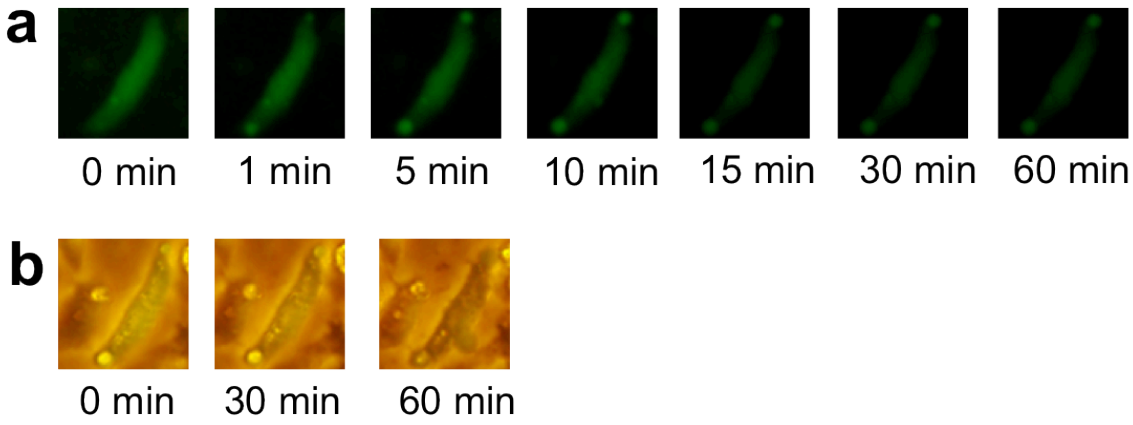

Fig. S8. Representative snapshot of a CHO cell bearing EGFP-145Amt1 gene upon adding 10 μM $CuSO_4$. a) fluorescence channel; b) wide field transmission.

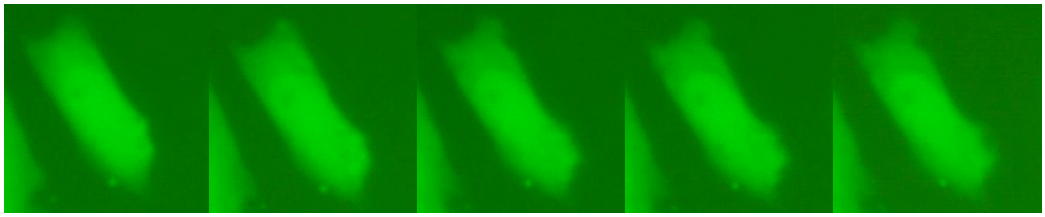

0 min 0.5 min 1 min 2 min 5 min

Fig. S9. The fluorescence changes of a CHO cell transfected by the plasmid containing EGFP at different time points after adding 1 mM Cu^{2+} to the medium.

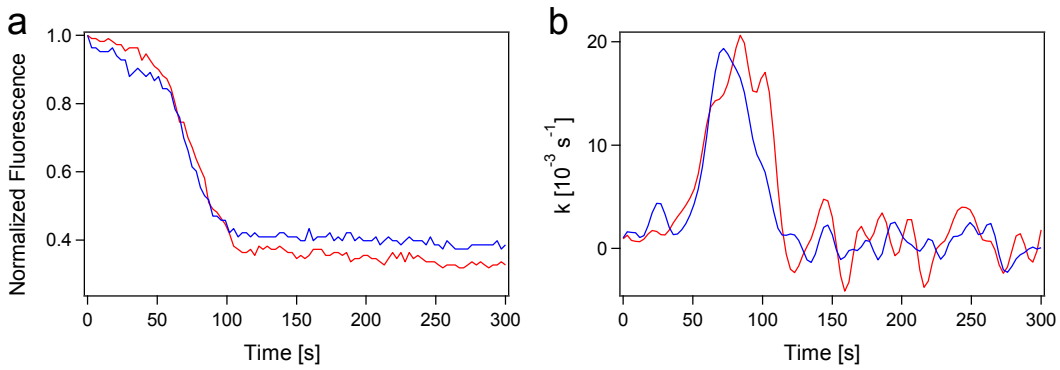

Fig. S10. Normalized fluorescence change of CHO cell transfected by the plasmid containing sensor protein over time at two different spots (a) and their corresponding fluorescence change rate (b). It is worth noting that the fluorescence change rate in this cell reaches maximum at ~80 seconds, different from the cell in Fig. 4.